Helvetica Physica Acta
Vol. 62 (1989)
0018-0238/89/070691-05$1.50+0.20/0

MONTE CARLO SIMULATION OF ULTRAFAST PHENOMENA

P. Lugli , Dipartimento di Ingegneria Meccanica, II Università di Roma
Via O. Raimondo, 00173 Roma, Italy

Abstract: A Monte Carlo study of ultrafast phenomena in polar semiconductors is presented, focusing on the relaxation of photoexcited carriers in bulk GaAs, InP, and in AlGaAs/GaAs quantum wells. The time scales associated with intercarrier interaction and carrier-phonon scattering are discussed. Very good agreement with time resolved experimental results is found.

1. Introduction

The Monte Carlo (MC) [1] approach has proven to be the most effective tool for the theoretical study of ultrafast phenomena in semiconductors [2]. In the following we will concentrate on the relaxation of photoexcited carriers in polar semiconductors, reviewing some of the existing work on the subject, and focusing on the microscopic phenomena that are involved with transport in a subpicosecond time scale. A comparison will be given with time resolved experimental results [3-5]. In a photoexcitation experiment, the energy put in the carrier system by the exciting radiation flows to, within and out of the coupled carrier-phonon system. Such system is very complex. Phonons might be driven out of equilibrium by the relaxing carriers, which in general will be of several types: electrons in different conduction band valleys (Γ, L, and X), holes in the three valence bands. Depending on the material, on the excitation level and on temperature, different types of carriers, lattice modes and carrier-phonon coupling will dominate the overall energy transfer from the external laser field into the lattice. We will concentrate on specific issues associated with ultrafast phenomena, in particular the possibility of LO phonon perturbations, the importance of intervalley transfer, and the influence of carrier-carrier scattering.

2. The Monte Carlo Simulation

The Monte Carlo results that will follow are based on a two-valley (Γ and L) model for GaAs. The following scattering mechanisms are considered (a complete description can be found in [6-7]: deformation potential coupling to acoustic phonons, treated exactly; unscreened polar optical coupling to LO phonons; unscreened scattering from ionized impurities, treated in the Conwell-Weisskopf formalism; deformation potential coupling to

intervalley $\Gamma \rightarrow L$ phonons; electron-electron scattering between Γ-valley electrons (a detailed description will be given below). The laser excitation is reproduced by adding particles to the simulation, distributed in time according to the lineshape of the laser pulse. In the simplest model, electrons are excited in the conduction band centered around a given energy E_{inj}, with a small broadening depending on the width of the laser pulse (typically around 20 meV). When the details of the band structure are taken into account for the photoexcitation process, the energy distribution of the photoexcited electrons is characterized by three distinct peaks, corrispondent to transitions from the three hole bands, slightly broadened because of the warping of the valence band and of the natural absorption linewidth.

Hot phonons

During the simulation, the LO-phonon distribution function is followed in its time evolution, and phonon-induced modifications to the relaxation rates of the electrons are considered [6-7]. The time evolution of the LO-phonon distribution $N_{\mathbf{q}}$ is calculated as a function of wavevector $\mathbf{q}$ from the Monte Carlo simulation , by setting up a histogram defined over a grid in q-space. After each scattering event involving an LO phonon, the histogram is updated. At fixed times during the simulation , the phonon distribution N_q is calculated accounting for phonon decays due to phonon-phonon processes. To account for the modifications induced by the phonon disturbance on the rate of electron-phonon scatterings, the integrated scattering probabilities for LO-phonons are calculated and tabulated at the beginning of the simulation using an artificially high value N_{max} for the phonon distribution. The choice of the final state of each scattering process involving an LO phonon is made using a rejection technique which compares the actual value of the differential scattering rate with the maximized one.

Carrier-carrier scattering

Within the ensemble Monte Carlo approach, carrier-carrier scattering is usually treated in the statically screened approximation for the coulomb interaction. The screening parameter and the scattering rates can be calculated directly from the simulated ensemble [9]. No assumptions on the form of the distribution function are required. Furthermore, the approach is not limited to steady-state situations, but applies as well to the study of transient phenomena.

3. Carrier Relaxation in Polar Semiconductors

The MC algorithm described earlier has been used to analize the luminenescence spectra after photoexcitation with a 400 fs wide laser pulse [4]. Only electron-electron

scattering for the Γ valley was considered. Figure 1 shows the M.C. electron distribution at three different time delays in bulk InP and GaAs. Some important differences are worth noticing. In GaAs, around 60% of the photoexcited carriers transfer to the satellite valleys during the laser pulse (the average time for $\Gamma \rightarrow L$ transition via phonon emission or absorption is around 80 fs). This creates the depletion in the high-energy region, above 0.3 eV, noticable in Fig. 1. Carriers return slowly to the Γ valley, with a characteristic

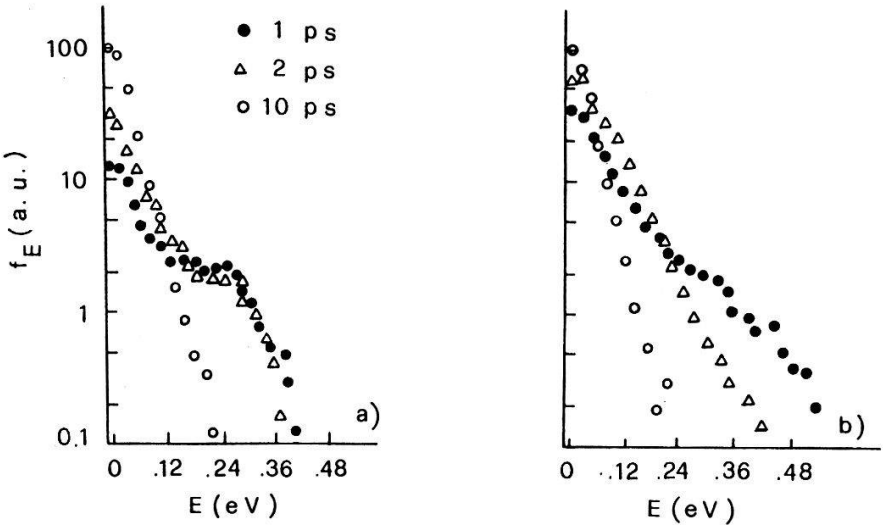

Fig. 1. Energy distribution function for Γ-valley electrons in GaAs (a) and InP (b) at three different time delays after the excitation. The excitation density is $5 \times 10^{16}\ cm^{-3}$ and the lattice temperature is 300 K.

time 2 or 3 ps. The net $\Gamma \rightarrow L$ transfer is actually a complicated series of processes where electrons can scatter in and out of the L valleys before leaving the actively-coupled energy region (that is the range of energy above 0.27 eV). The L valleys in InP sit at a much higher energy, and do not significantly contribute to the cooling process. The electron distribution is smoother than in GaAs, and the population of the low-energy region is higher at all times, since the cooling process is not slowed down by intervalley transfer. In both cases, electrons are characterized at the shortest time (1 ps) by an athermal distribution. Even if the intercarrier scattering is not sufficiently strong, at the low densities considered here ($5 \times 10^{16} cm^{-3}$), to assure complete thermalization within the ensemble, it is nevertheless sufficient to smooth out the initially peaked distribution. Time resolved luminescence spectra have been calculated using the electron distribution function shown before, and assuming equilibrium conditions for the holes. A very good agreement has been found with the experimental data for a $\Gamma - L$ deformation potential $D_{\Gamma L}$ of $6.5 \pm 1.5 \times 10^8\ eV/cm$ [4]. The characteristic behaviour of the two materials also shows up in the non-equilibrium LO phonon distributions shown in Fig. 2. A stronger and faster phonon build up is found in InP, with the maximum amplification reached at time delay of 1 ps. The presence of non equilibrium phonons results in a density dependence of the electron cooling rate, which is reduced at high electron concentration due to phonon reabsorption.

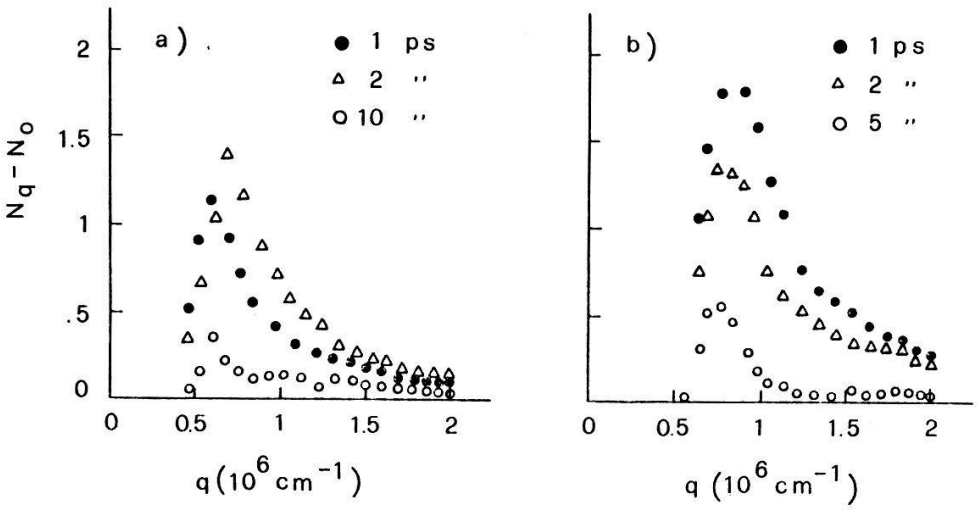

Fig. 2. LO-phonon distribution for Γ-valley electron in GaAs (a) and InP (b) for three different time delays after the excitation at T_L=300 K.

The MC algorithm was also applied to a single quantum well of GaAs-AlGaAs, with subband energies given by the solution of the one dimensional wave equation for a square well potential. Details of the method can be found in [11,12]. The electrons were allowed to interact via a statically screened coulomb interaction determined by the long wavelength limit of the two-dimensional Lindhard dielectric function. As for the bulk case, a reduction of the electron cooling rate was observed due to the reabsorption of nonequilibrium phonons which build up during the initial pumping and the first stage of the electron relaxation. The effect is stronger when a considerable number of electrons have relaxed to the low energy region below the emission threshold. A MC analysis has also been performed of pump-and-probe time resolved experiments at low excitation energies [5]. The experimental results indicate that an internal thermalization of each component of the excited plasma is achieved in about 200 fs. Becuase of the low pump energy, the excess electron and hole energies lie below the threshold for optical phonon emission. The fast relaxation is then attributed to the effect of intercarrier scattering. For the MC simulation, both e-e and e-h scattering were considered [13,14]. The calculated electron distribution function before and after the excitation by a 100 fs laser pulse (centered at t=0 fs) is shown in Fig. 3. A 95 A wide undoped quantum well is used, with an injected density of $2x10^{10}cm^{-2}$ carriers.

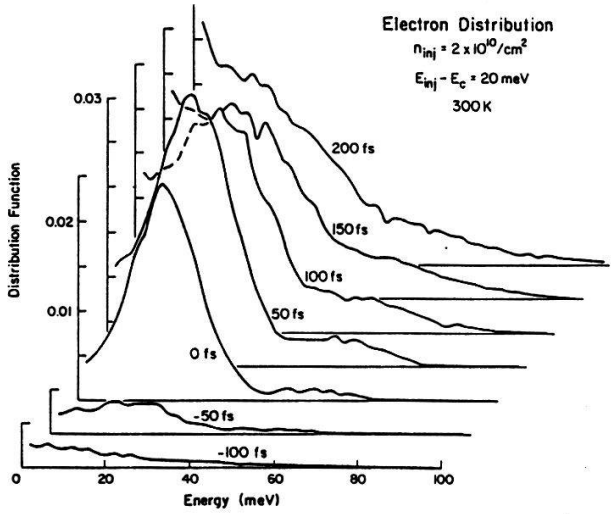

Fig. 3. Electron energy distribution for a GaAlAs/GaAs quantum well before and after a 100 fs pulse centered at $t = 0$.

The excess electron energy in the conduction band is taken as 20 meV, with a 20 meV broadening associated with the spectral width of the pulse. The observed time evolution of the electron distribution closely resembles the one found experimentally in the differential transmission; that is an athermal carrier distribution develops at the peak of the pulse and subsequently relaxes to a Maxwellian shaped distibution after 200 fs. At intermediate times, a slight bump is observed at higher energies of the electron distribution, which is connected to optical phonon absorption. The MC analysis of the time evolution of the electron and hole distributions shows that the experimental spectra are mainly determined by the electron dynamics. The observed thermalization is controlled by e-e interaction, with the inelastic e-h scattering playing a minor role.

4. Conclusions

We have presented several applications of the MC method to the study of the relaxation of photoexcited carriers in polar semiconductors. Good agreement with experimental results is found. Non-equilibrium phonons effects can be of great importance expecially at low temperatures, high excitation energies, and high injected carrier densities. Carrier-carrier scattering is the fastest randomizing mechanism, and leads at the internal thermalization of the photoexcited plasma in a femtosecond time scale even at moderate densities.

5. References

[1] C. Jacoboni and L. Reggiani, Rev. Mod. Phys., **55**, 645 (1983).
[2] P. Lugli, Physica Scripta, **T19**, 190 (1987).
[3] J.A. Kash, J.C. Tsang and J.M. Hvam, Phys. Rev. Lett. **54**, 2151 (1985).
[4] J. Shah, B. Deveaud, J.C. Damen, W.T. Tsang, A.C. Gossard and P. Lugli, Phys. Rev. Lett. **59**, 2222 (1987).
[5] W.H. Knox, D.S. Chemla, and G. Livescu, Solid State Electron. **31**, 425 (1988).
[6] P. Lugli, Solid State Electron. **31**, 667 (1988).
[7] P. Lugli, P. Bordone, L. Reggiani, M. Rieger, P. Kocevar and S. Goodnick, Phys. Rev. B., to be published.
[8] P. Lugli, C. Jacoboni, L. Reggiani, and P. Kocevar, Appl. Phys. Lett. **50**,1251 (1987).
[9] M.A. Osman, and D.K. Ferry, Phys. Rev. **B36**, 6018 (1988).
[10] P. Lugli, in "Band Gap Engineering in Semiconductor Microstructures", Ed. R.A. Abram and M. Jaros, p. 187 , Plenum Press, New York (1988).
[10] P. Lugli and D.K. Ferry, Physica **134B**, 364 (1985).
[11] P. Lugli and S. Goodnick, Phys. Rev. Lett. **59**, 716 (1987).
[12] S. M. Goodnick, and P. Lugli, Phys. Rev. **B37**, 2578 (1988).
[13] S. M. Goodnick, and P. Lugli, Solid State Electron. **31**, 463 (1988).
[14] S.M. Goodnick and P. Lugli, Phys Rev. **B14**, 3014 (1988).
[15] P. Lugli, D. K. Ferry, Phys. Rev. Lett. 56, 1295 (1986).
[16] P. Lugli, L. Reggiani, in "Noise in Physical Systems and 1/f Noise", Eds. A. D'Amico and P. Mazzetti, Elsevier Science Publisher B.V., p. 235 (1986).